4ICEGE Thessaloniki-GREECE 2007

4th International Conference on
Earthquake Geotechnical Engineering
June 25-28, 2007
Paper No. 1195

QUANTIFICATION OF SEISMIC SITE EFFECTS IN TWO-DIMENSIONAL IRREGULAR CONFIGURATIONS

Chloé ARSON[1], Behrouz GATMIRI[2]

ABSTRACT

The response of a site to a seismic solicitation depends on local topography and geotechnical characteristics. Current building codes, based on 1D models of soil columns, do not take 2D phenomena into account to estimate these site effects. This work aims at quantifying the combined effects of geometry and stratigraphy in sedimentary basins subjected to synthetic SV waves of vertical incidence. The main purpose of this paper is to elaborate a predictive method to estimate horizontal ground movements (ux) in two-dimensional irregular configurations. Extensive parametric studies are done by means of an optimised hybrid numerical technique combining finite and boundary elements. Considering a reference station on the outcrop, the ratio ux/ux(ref) is broken down into a product of various factors. Each coefficient represents a site effect parameter: offset (x/L); filling (H_1/H); depth (H/L); slope (α) and shape (ellipsoid or trapezium). The topographical and geotechnical variables controlling 2D site effects are evaluated separately in order to identify the predominant parameters. Specific 2D effects are also characterized by a simplified breakdown requiring a unique "2D Combined Amplification" coefficient (2DCA coefficient).

Keywords: site effect; prediction; characteristic coefficients; building codes; hybrid numerical method

INTRODUCTION

After destructive earthquakes occurring in mountain areas, buildings located at the top of cliffs or hills usually suffer much more intensive damage than those located at the base. For example, the 1995 Kozani earthquake in Greece particularly affected villages built on hills. In 1985, damages stated after the Mexico earthquake gave evidence of the influence of the sedimentary basin on the seismic response of the site. Measurements and experimentations showed the influence of topographical and geotechnical local characteristics on the ground motion responding to a seismic solicitation [Trifunac and Hudson, 1971; Nechtschein et al., 1995]. This phenomenon is accounted for "site effects". A state of the art about site effects is done in [Faccioli et al., 2002; Reinoso et al., 1997].
Various numerical techniques have been used to study site effects, like the finite difference method [Boore et al., 1981; Ohtsuki and Karumi**,** 1983], the finite element method [Castellani et al., 1982; Bielak et al., 1999], the discrete wavenumber method [Bard, 1982; Kawase, 1988], and the boundary element method [Wong and Jennings, 1975; Sanchez-Sesma et al., 1982; Luco and Barros, 1995; Reinoso et al., 1997]. The ground movement amplifications predicted by 1D models of soil columns subjected to seismic solicitations are currently used in building codes. But many parametric studies give evidence of the existence of specific 2D and 3D effects, inferring greater amplifications than in 1D configurations. Particularly, Bard and Bouchon defined a 2D resonance [Bard and Bouchon, 1985]. As the quantitative predictions of 3D simulations are close to 2D ones, site effects are usually studied in two dimensions, to get realistic results by means of time-saving computations.

[1] Centre d'Enseignement et de Recherche en Mécanique des Sols (CERMES), Ecole Nationale des Ponts et Chaussées (ENPC), France, Email: chloe.arson@wanadoo.fr
[2] University of Tehran, Iran, and Ecole Nationale des Ponts et Chaussées (ENPC), France

In this paper, a hybrid numerical technique, combining finite elements in the near field and boundary elements in the far field, is used to lead an extensive parametric study of two-dimensional wave scattering due to incident SV waves. Site effects in sedimentary valleys are mainly studied through landscape characters: sedimentary filling ratio, depth, inclination slope angle, shape and offset. An evaluation technique of horizontal displacement amplifications is developed by means of a product of characteristic factors. The aim of this predictive method is to separate, to qualify and to quantify the contributions of the main parameters to 2D site effects. The reasoning followed is similar to the one usually developed in civil engineering building codes concerning the construction and the use of safety coefficients.

NUMERICAL METHOD

Combination of FEM and BEM

In this study, sediments are modelled by finite elements ("zone 1" of the model in the following). Substratum is represented by boundary elements ("zone 2"), which is adapted to the study in the far field. The region of interest is a half-space and must thus be enclosed with fictitious boundary elements known as "enclosing elements". All materials are supposed to be elastic.

FEM

In the finite-element domain, applying the modified Newton-Raphson iterative method leads to:

$$M \bullet \ddot{U}^{t+\Delta t(k)} + K^t \bullet (U^{t+\Delta t(k)} - U^{t+\Delta t(k-1)}) = R^{t+\Delta t} - F^{t(k)} \quad (1)$$

where M is the mass matrix, and K^t is the rigidity matrix at instant t. $U^{t+\Delta t(k)}$ is the displacement vector for the k[th] iteration done to reach the load increment $R^{t+\Delta t}$ imposed at t+Δt. $F^{t(k)}$ is the force calculated by the behavior law of the material at the k[th] iteration.

Using the Newmark method in which:

$$U^{t+\Delta t} = U^t + \frac{\Delta t}{2} \cdot (\dot{U}^t + \dot{U}^{t+\Delta t}) \quad (2)$$

and adding $\overline{K}^t \bullet U^{t+\Delta t(k-1)}$ to both sides of equation (1), it is found that:

$$\overline{K}_1^t \bullet U^{t+\Delta t(k)} = R_1^{t+\Delta t} - Z_1^{t+\Delta t(k)} \quad (3)$$

where:

$$Z_1^{t+\Delta t(k)} = F_1^{t(k)} - K_1^t \bullet U_1^{t+\Delta t(k-1)} - \left(\frac{4}{\Delta t^2} \cdot U_1^t + \frac{4}{\Delta t} \cdot \dot{U}_1^t + \ddot{U}_1^t \right) \bullet M_1 \quad (4)$$

BEM

The boundary integral equation of elastodynamics in time-domain for a homogeneous isotropic elastic medium, occupying a volume Ω, bounded by a surface Γ, and subjected to an incident plane wave is:

$$c_{ij}(\xi) \cdot u_j(\xi) = \int_\Gamma \left[G_{ij}(\xi,\chi,t) * t_j(\chi,t) - F_{ij}(\xi,\chi,t) * u_j(\chi,t) \right] \cdot d\Gamma + u_i^{eq}(\xi,t) \quad (5)$$

if the contributions of initial conditions and of body force are neglected. ξ is the source point, χ is the field point; u_i and t_i are the amplitudes of the *i*-th component of displacement and traction vectors respectively, at the boundary; u_i^{eq} represents the incident wave; symbol * indicates a Riemann convolution integral; c_{ij} is the discontinuity term depending on the local geometry of the boundary at ξ and on the Poisson's ratio; G_{ij} and F_{ij} are the fundamental solutions representing the displacement and traction at χ in direction *i* due to a unit point force applied at ξ in the *j*-direction.

Numerical implementation of equation (5) requires a discretization in both time and space. For this purpose, the boundary Γ is discretized into a defined number of elements, and time axis is divided into *N* equal intervals so that t=N.Δt. In this work, quadratic spatial variation of the field variables (displacement and traction) is assumed over each element. Both constant and linear temporal

variations can be used for each field variable. Space discretization gives the following matricial expression at instant t=N.Δt:

$$F^1 \bullet U^N = G^1 \bullet T^N + \sum_{n=1}^{N-1} \left(G^{N+1-n} \bullet T^n - F^{N+1-n} \bullet U^n \right) \quad (6)$$

FE/BE coupling

FE-equations are expressed in force and displacement whereas in the BEM, stresses replace forces. Equations need thus to be adapted. In the last term of (6), stresses are transformed into forces as follows:

$$Z^{t(k)} = N \cdot \left(G^1 \right)^{-1} \bullet \sum_{n=1}^{N-1} \left(F^{N+1-n} \bullet U^n - G^{N+1-n} \bullet T^n \right) \quad (7)$$

Zone 2 (substratum modelled by boundary elements) has a common frontier with zone 1 (sediments modelled by finite elements). The governing matricial equation of zone 2 can thus be written in the same way as (4):

$$\overline{K}_2^t \bullet U_2^{t+\Delta t(k)} = R_2^{t+\Delta t(k)} - Z_2^{t+\Delta t(k)} \quad (8)$$

Validation of HYBRID program

The above formulation is integrated in a BEM/FEM software (HYBRID), which was developed and validated by Gatmiri and his coworkers. In the far field, the model is based on the direct boundary integration technique [Gatmiri and Kamalian, 2002a]. The boundary elements are combined to finite elements, used for the near field representation. Two-dimensional fundamental solutions have been found out and implemented in HYBRID [Gatmiri and Kamalian, 2002b, Gatmiri and Nguyen, 2005].
The integration process has been optimised in the domain by time truncation [Gatmiri and Dehghan, 2005]. Precision is controlled by two parameters: a number of time steps which gives the backtracking limit, and a tolerance coefficient that cuts the calculation when the terms become negligible. This numerical technique is fast and accurate. Moreover, artificial waves generated at the truncation points of the model vanish easier if the optimised method is used.

IDENTIFICATION, DISCRIMINATION AND PREDICTION OF 2D SITE EFFECTS

Presentation of the model

In this work, numerical simulations have been done on sedimentary valleys modelled in two dimensions, with HYBRID program. The results have been analysed by comparison to former parametric studies done with the same program [Nguyen and Gatmiri; Nguyen, 2005]. Ratios have been defined in order to find out a relevant calculation method of horizontal ground movements. The aim of this approach is to provide a quantitative prediction of horizontal superficial displacements without using numerical computations, which could be useful for civil engineering purposes.
Displacement amplification is defined as *ux/ux(ref),* where *ux(ref)* is the horizontal displacement observed at the surface of a half-space made of rock. It is as if the reference station was on the distant outcrop. The incident signal is a Ricker SV wave propagating vertically. The amplification of the input signal is fixed to unit and the predominant frequency f_c is equal to 2 Hz. Materials are assumed to be dry and linear elastic (See Tab. 1). The main geometrical parameters are defined on Fig. 1.
Two shapes are studied for the alluvial basin: trapeziums (for H_1/H = 0 ; 1) and truncated ellipses (for H_1/H = 0 ; 0,25 ; 0,5 ; 0,75 ; 1). (H/L ; L_1/L) combinations chosen for the study are summed up in Tab. 2. The present work only deals with observation points located in the basin. The response of the neighbouring outcrop is not studied.

Table 1. Mechanical parameters of the materials

	E (MPa)	ν	ρ (kg/m^3)	c (m/s)
soil	900	0,3	1630	465
rock	6720	0,4	2450	1000

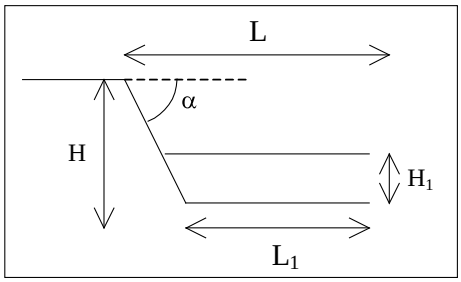

Figure 1. Main geometrical parameters characterizing the alluvial basins. Due to symmetries, only the half of the valley is represented.

Table 2. Values of depth and width at the basis chosen in the parametric studies, and corresponding values of inclination angle

L_1/L	H/L			
	0,2	0,4	0,6	1
0	11,31°	21,80°	30,96°	45,00°
0,4	18,43°	33,69°	45,00°	59,04°
1	90,00°	90,00°	90,00°	90,00°

A product of characteristic coefficients

Topographical and geological respective contributions to horizontal ground motion amplification are separated by means of a product of five significant coefficients. The factors represent the influence of parameters controlling site effects: offset (*x/L*); filling (H_1/H); depth (*H/L*); inclination angle of the slope (α); shape of the basin (trapezium or truncated ellipse).

$$\frac{ux}{ux_{ref}} = \frac{ux^*}{ux^*(0,-(H-H_1))} \cdot \frac{ux^*(0,-(H-H_1))}{ux^*(0,-H)} \cdot \frac{ux^*(0,-H)}{ux^*(L,0)} \cdot \frac{ux^*(L,0)}{ux^*(L_1,-H)} \cdot \left[\frac{ux}{ux^*} \cdot \frac{ux^*(L_1,-H)}{ux_{ref}} \right] \quad (9)$$

- Offset coefficient: $$\frac{ux^*}{ux^*(0,-(H-H_1))} = f\left(\frac{x}{L}, \frac{H_1}{H}\right) \quad (10)$$
- Filling coefficient $$\frac{ux^*(0,-(H-H_1))}{ux^*(0,-H)} = f\left(\frac{H_1}{H}\right) \quad (11)$$
- Depth coefficient $$\frac{ux^*(0,-H)}{ux^*(L,0)} = f\left(\frac{H}{L}\right) \quad (12)$$
- Slope coefficient $$\frac{ux^*(L,0)}{ux^*(L_1,-H)} = f(\alpha) \quad (13)$$
- Shape coefficient $$\frac{ux}{ux^*} \cdot \frac{ux^*(L_1,-H)}{ux_{ref}} = f\left(shape, \frac{x}{L}, \frac{H}{L}\right) \quad (14)$$

Offset, filling, depth and slope coefficients are assumed to be independent from the shape of the topography. These four ratios are calculated on truncated ellipses and applied to every configuration. That is why they are marked with *. The correction is done through the shape factor. The shape factor is equal to one for truncated ellipses, and must be calculated from formula (14) in other cases. If L_1/L = 1, the valley is rectangular whatever the chosen basin shape is. Offset, filling, depth and slope coefficients are always equal to the ones obtained for truncated ellipses. The shape coefficient can be considered one, and no more assumption is necessary. As exposed in [Nguyen, 2005; Nguyen and Gatmiri], for other values of L_1/L, ellipsoidal configurations give intermediate responses for both empty and full valleys. This trend could also be noticed in the simulations done for this study. Ellipsoidal shapes are thus representative. Variables controlling filling, depth and slope have been separated, so the corresponding coefficients depend on an only parameter (11; 12 and 13). For a given abscissa *x/L*, filling ratio H_1/H determines the type of material on which the superficial observation point is located. That is why the offset coefficient (10) does not only depend on *x/L*, but also on H_1/H parameter, which introduces a second dimension in the definition of the geometrical location of the

observation point. The shape coefficient varies with three geometrical parameters, in order to make it representative of the influence of the curvature of the slope.

Offset coefficient

Horizontal displacements are calculated on regularly spaced points at the surface of ellipsoidal basins. For each filling ratio H_1/H, the maximal value obtained for the offset coefficient (10) among all the (H/L ; L_1/L) combinations is retained. Fig. 2 represents the corresponding curves.

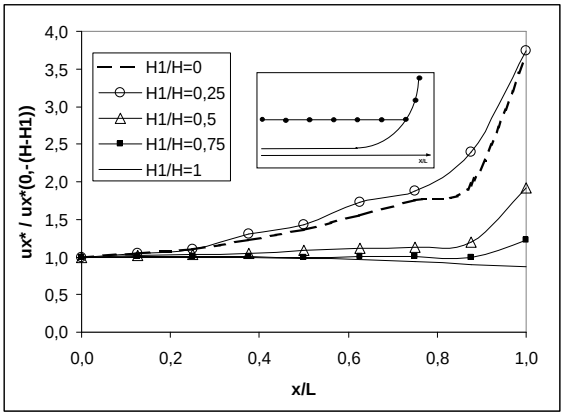

Figure 2. Offset coefficient curves

If the valley is full (H_1/H = 1), the horizontal surface displacement reaches a maximum at the centre of the basin. That is why offset is an attenuation factor. Partially filled valleys manifest a topographical effect on the top part of the slope. It tends to amplify horizontal displacements. The width of the domain submitted to topographical effects increases as filling decreases. Offset is thus an amplification factor. Amplification rises if the sedimentary layer is thin or if x/L is close to one. At the edge, the offset ratio is equal to 1,8 if H_1/H = 50% and to 3,7 if H_1/H = 25%. The biggest offset ratios are obtained for H_1/H = 25%, and not for H_1/H = 0%, as could be expected. In fact, site effects seem to be "more topographic" in the H_1/H = 25% case than in the H_1/H = 0% case.

Filling coefficient

As for the offset ratio, the filling coefficient (11) is calculated in every configuration, and for a fixed filling ratio H_1/H, the maximal value obtained among all the (H/L ; L_1/L) combinations is retained. Fig. 3 represents the corresponding graph.

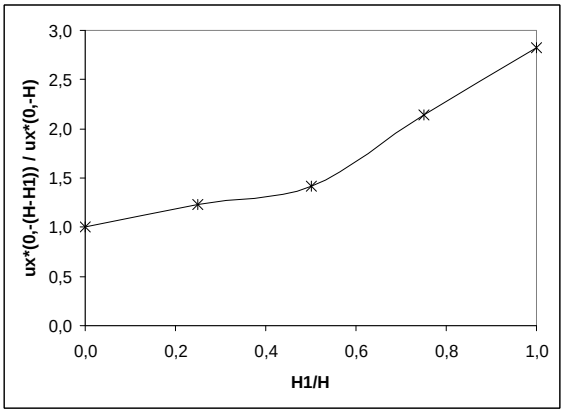

Figure 3. Filling coefficient curve

The filling coefficient represents a mere 1D geological effect. The fundamental resonance frequency of a H-thick sedimentary layer is noted f_{h0}:

$$f_{h0} = \frac{c_S}{4 \cdot H} \quad (15)$$

where c_S is the shear waves velocity of sediments. Without damping, calculations at the resonance a soil column yield to a maximal amplification of horizontal displacements reaching $1/\beta$, where β is the impedance ratio:

$$\beta = \frac{\rho_S \cdot c_S}{\rho_R \cdot c_R} \quad (16)$$

ρ_S and ρ_R are the volumetric masses of sediment and rock respectively; c_S and c_R are the shear waves velocities of sediment and rock respectively. In our models, β = 0,31, so that the maximal amplification expected is 3,22. This threshold is never reached. Consequently, the soil column located at the centre of the basin never enters in 1D resonance. 1D fundamental frequencies f_{h0} (15), calculated for every configuration, are given in Tab. 3.

The configurations in which the predominant frequency of the incident signal (f_c = 2Hz) is the closest to the 1D fundamental frequency correspond to the most filled valleys. Due to the position relative to the amplification peak at resonance, basins with high filling ratios are thus more susceptible to amplify central horizontal displacements. This induces larger filling coefficients. This statement explains why the filling coefficient increases with the filling ratio H_1/H (Fig. 3). In all cases, the filling coefficient is an amplification factor.

Table 3. 1D fundamental frequencies of the soil columns located at the centre of the studied valleys

H_1/H	0	0,25	0,5	0,75	1
H/L=0,2	X	23,24	11,62	7,75	5,81
H/L=0,4	X	11,64	5,82	3,88	2,91
H/L=0,6	X	7,84	3,92	2,59	1,94
H/L=1	X	4,64	2,32	1,55	1,16

Depth coefficient

The calculation method is similar to the one of the filling coefficient. The depth coefficient (12) is calculated in every configuration. For each value of *H/L*, the maximal value obtained among all the (L_1/L ; H_1/H) combinations is retained. The depth coefficient is defined as the ratio of horizontal displacements calculated on a point of substratum and horizontal displacements calculated at the edge of the valley. To study depth effects, it is more natural to study horizontal displacements on a point of the surface relatively to those at a point of substratum. That is why Fig. 4 represents the inversed depth coefficient.

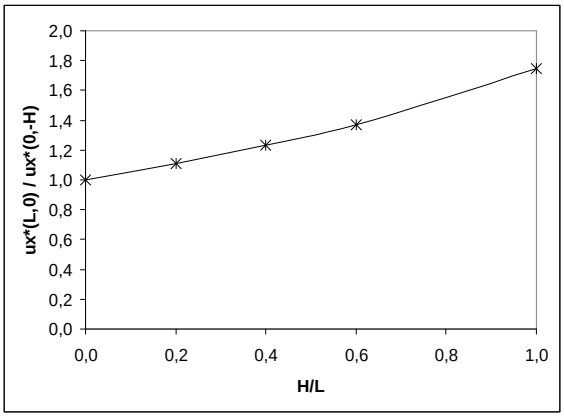

Figure 4. Inversed depth coefficient curve

The simulations done for this study showed that the influence of sediments tends to dominate topographical effects when the thickness of the alluvial layer exceeds 0,2L. The amplification of surface displacements rises with the absolute thickness of the sedimentary layer.

As announced in the introduction, the influences of the parameters controlling site effects have been separated. The depth coefficient only relates the effect of depth. For each depth, the maximal amplification computed among the studied configurations was retained in order to give safe estimations of amplifications. Due to the choice of construction of the depth coefficient, an increase of the absolute thickness of the sedimentary layer is translated by an increase of depth on Fig. 4.
That is why the inversed depth coefficient increases with depth, which does not infer that the amplification of displacements always grow with depth. Moreover, horizontal displacements calculated at the edge of valleys are systematically amplified. It could thus be expected that the inversed depth coefficient would be more than the unit. As a consequence, the inversed coefficient is always an amplification factor. This means that in the breakdown (9), the depth coefficient is an attenuation factor.

Slope coefficient
For a given inclination angle α, the maximal slope coefficient (13) calculated for the whole (H/L ; L_1/L ; H_1/H) combinations is retained. The curve is shown on Fig. 5.
In the construction of the slope coefficient (13), geotechnical effects vanish due to the maximization on α. Overestimation of slope amplification rises to a maximum of 2,3 times the amplifications calculated by numerical simulation. The scale of order is thus preserved. This means that the slope coefficient really represents a mere topographical aspect of site effects. Parametric studies done on empty canyons [Nguyen, 2005; Nguyen and Gatmiri] show that displacement amplifications get stronger as the slope become more severe. The increase of the slope coefficient with α reflects this trend (Fig. 5).

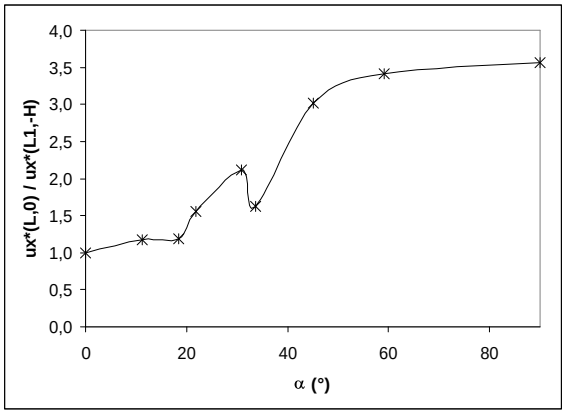

Figure 5. Slope coefficient curve

Topographical effects are mainly caused by:

- wave focusing in convex relieves;
- interferences between incident and reflected volume waves with diffracted surface waves.

If embankment is low, surface waves get late relatively to volume waves. Interferences have thus less chance to occur. Moreover, convexity rises with embankment, thus with α. In other words, an increase of the slope coefficient is expected when:

- α increases;
- H/L increases at a fixed value of L_1/L;
- L_1/L decreases at a given value of H/L.

The last two statements can explain why the increasing of the slope coefficient is not monotonous. Indeed, the coefficient is weaker for 34° than for 31°. In the parametric study (See Tab. 2), the 31° inclination angle corresponds to the (H/L = 0,6 ; L_1/L = 0) configuration, and the 34° angle refers to (H/L = 0,4 ; L_1/L = 0,4). Both angles are very close. The determining parameter is thus the width at the base of the valley (L_1). In the (H/L = 0,4 ; L_1/L = 0,4) configuration, the slope is steeper, but the opening at the base works against the expected amplification.

As recalled for the depth coefficient, horizontal displacements at the edge of valleys are always amplified. Therefore, it is not surprising to find that the slope coefficient is more than the unit (See (13)). For all cases, the slope coefficient is thus an amplification factor.

Shape coefficient

In this parametric study, only one shape coefficient has been considered, since only one shape has been modelled in addition to the ellipsoidal reference configuration (See (14)). Shape represents a mere topographical effect. That is why the determination of the shape coefficient is based on the comparison of empty trapezoidal and ellipsoidal canyons of the same dimensions (for H/L and L_1/L). Only the horizontal displacements calculated for $L_1/L = 0{,}4$ are used for the calculation. In other words, H_1/H and L_1/L are fixed. The shape coefficient depends only on x/L and H/L. To find out ux/ux^*, displacements are evaluated on regularly spaced observation points at the surface of both canyons. The resulting graphs are given on Fig. 6.

Variations of the shape coefficient increase with depth. Shifting from an ellipsoidal configuration to a trapezoidal shape induces an attenuation of horizontal surface displacements. The attenuation is minimal at the centre (about 0,8) and maximal at the edge (down to the half of the amplifications obtained for truncated ellipses).

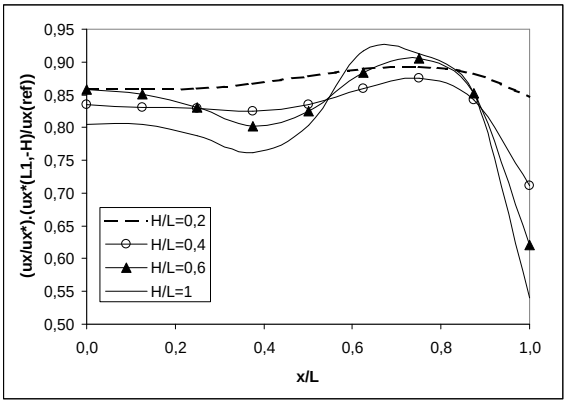

Figure 6. Shape coefficient curves obtained from trapezoidal configurations

Simplification: a unique "2D Combined Amplification" coefficient (2DCA coefficient)

Generally speaking, calculations on 1D site effects are mastered. The preceding paragraph presents a predictive evaluation method of horizontal displacements for 2D models. This paragraph aims at developing a simplified technique based on a unique "2D Combined Amplification" coefficient (2DCA coefficient). It is assumed that horizontal displacement at the centre of the valley is known. In engineering problems, this is generally the case. $ux(0,-(H-H_1))/ux(0,-H)$ can indeed be evaluated by means of a 1D column model with moderate errors. The objective is to build a coefficient that could sum up the influence of the second dimension in the model. 1D models are based on vertical analyses. That is why the 2DCA coefficient must depend on x/L. The offset coefficient (10) meets this condition. As for the preceding breakdown (9), it is assumed that ellipsoidal configurations can be set as references. Consequently, the offset coefficient must be corrected by the shape coefficient (14). The resulting simplified breakdown is thus expressed as:

$$\frac{ux}{ux_{ref}} = \frac{ux\left(0,-(H-H_1)\right)}{ux\left(0,-H\right)} \cdot \frac{ux^*}{ux^*\left(0,-(H-H_1)\right)} \cdot \left[\frac{ux}{ux^*} \cdot \frac{ux^*\left(L_1,-H\right)}{ux_{ref}}\right] \tag{17}$$

- 1D amplification ratio $\dfrac{ux\left(0,-(H-H_1)\right)}{ux\left(0,-H\right)}$ (18)
- 2DCA coefficient $\dfrac{ux^*}{ux^*\left(0,-(H-H_1)\right)} \cdot \left[\dfrac{ux}{ux^*} \cdot \dfrac{ux^*\left(L_1,-H\right)}{ux_{ref}}\right] = f\left(\dfrac{x}{L}, \dfrac{H_1}{H}, \dfrac{H}{L}, shape\right)$ (19)

Comparing the two breakdowns (9) and (17), it can be seen that the simplification consists in eliminating the depth and slope coefficients, and to replace the reference filling coefficient (11) by an exact filling coefficient representing 1D effects (18). For truncated ellipses, the shape coefficient is equal to the unit, so that the "2D Combined Amplification" coefficient (2DCA coefficient) is similar to the offset coefficient (Fig. 2). For trapezoidal valleys, the aspect of the 2DCA coefficient curve strongly depends on the filling ratio H_1/H (Fig. 7). For empty canyons, the 2DCA coefficient is an amplification factor, increasing with offset (from 1 at x/L = 0 to 3 at x/L = 1). For full sedimentary valleys, it is an attenuation factor, varying only slightly with x/L (regularly decreasing from 0,8 at the centre to a minimum of 0,5 at the edge).

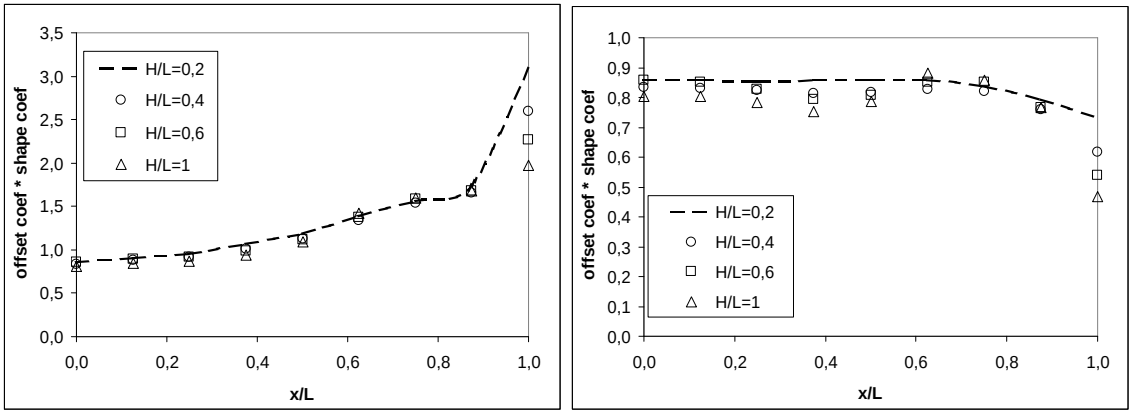

a. H_1/H = 0 **b. H_1/H = 1**

Figure 7. 2DCA coefficients for trapezoidal configurations: empty canyons (a) and full sedimentary valleys (b)

ACCURACY OF THE PREDICTION TECHNIQUES

Amplifications of horizontal displacements are calculated by three methods: numerical simulation, product in five coefficients (9), and breakdown using a single 2DCA coefficient (17). Results obtained through breakdowns are compared to those given by HYBRID:

$$\frac{\left(\frac{ux}{ux_{ref}}\right)_{decomposition}}{\left(\frac{ux}{ux_{ref}}\right)_{numericalsimulation}} \qquad (20)$$

The product of five factors (9) involves maximized ratios. Amplification is thus systematically over-estimated. In the simplified technique (17), the 1D amplification factor corresponds to an exact value. Moreover, the "2D Combined Amplification coefficient" (2DCA coefficient) can be attenuating for full valleys (Fig. 2 for truncated ellipses and Fig. 7.b for trapeziums). Therefore, the 2DCA coefficient method may lead to under-estimations. The performances of both predictive calculation methods are studied through:

- a comparison of over-estimations of *ux/ux(ref)* (Fig. 8 and 9);
- an evaluation of the under-estimation risks in the breakdown using the 2DCA coefficient (Fig. 10).

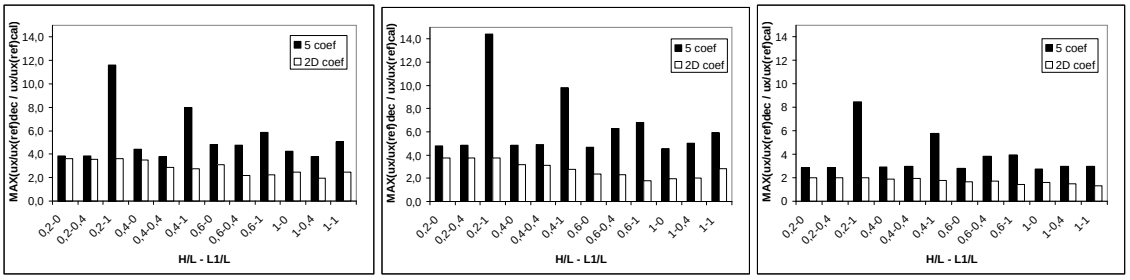

a. H_1/H = 0 **b. H_1/H = 0,25** **c. H_1/H = 0,5**

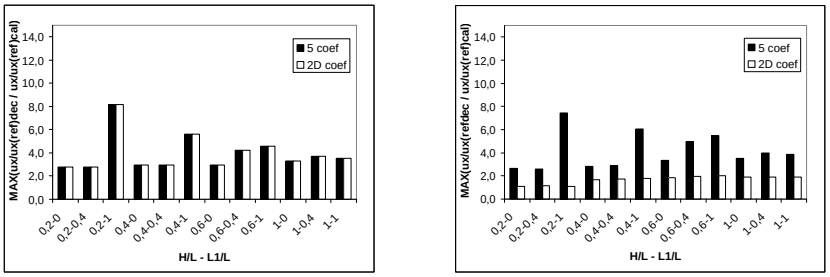

d. H_1/H = 0,75 **e. H_1/H = 1**

Figure 8. Maximal values of horizontal surface displacement amplifications provided by both predictive methods for truncated ellipses configurations

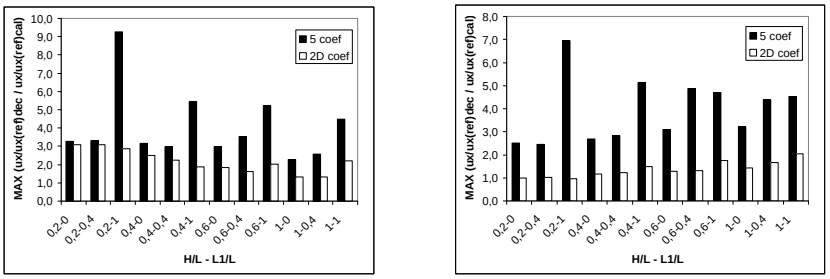

a. H_1/H = 0 **b. H_1/H = 1**

Figure 9. Maximal values of horizontal surface displacement amplifications provided by both predictive methods for trapezoidal configurations

Over-estimations provided by the 5-factor product are systematically higher than the ones given by the 2DCA coefficient method. It is normal, since in the first product (9), over-estimations are summed in five ratios, whereas the simplified technique (17) requires only three factors. The largest over-estimations deal with shallow rectangular valleys (H/L = 0,2 or 0,4 ; L_1/L = 1). The absolute error (20) rises up to 14 for truncated ellipses, and to 9 for trapeziums. Errors are greater on empty or poorly filled valleys (H_1/H = 0 or 0,25). The absolute error adds up to about 4 for the 5-factor product applied on truncated ellipses, whereas it is between 2 and 3 through the 2DCA coefficient method (Fig. 8.a and 8.b). In trapezoidal valleys, the error is about 3 with the 5-factor technique and 2 with the simplified method (9.a). When the sedimentary layer is thick (H_1/H = 0,75 or 1), the 2DCA coefficient technique is really more precise: the absolute error (20) is very close to the unit. On the contrary, the product of five factors over-estimates amplifications from 3 to 5 times in most cases (Fig. 8.d; 8.e and 9.b). Both techniques give the same accuracy on half-filled ellipsoidal valleys (Fig. 8.c).

The 2DCA coefficient evaluation technique is not so risky. Truncated elliptic valleys present no risk of horizontal displacement under-estimations (Fig. 10.a). For trapezoidal valleys, risks are nil for empty canyons, and weak for full valleys: the minimal absolute error (20) reaches 0,85 (Fig. 10.b). An exception is the deep empty rectangle (H/L = 1 ; L_1/L = 1 ; H_1/H = 0), for which the 2DCA coefficient predictive method evaluates horizontal displacement amplification to 60% of its value.

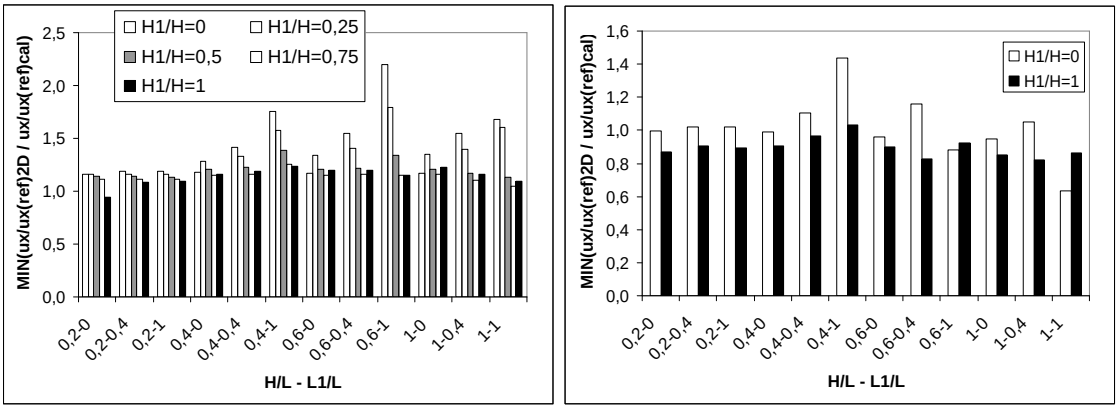

a. Truncated ellipses **b. Trapeziums**

Figure 10. Minimal values of horizontal surface displacement amplifications given by the 2DCA coefficient method

As a conclusion, the 2DCA coefficient (19) is relevant to estimate amplifications of horizontal displacements due to site effects. Over-estimations scarcely exceed twice the value calculated by a numerical method. Risks of under-estimations are not so significant. It is possible to get a good approximation of amplifications by applying a security coefficient of about 1,25. Though, the physical interpretation of the 2DCA coefficient must be considered cautiously. In fact, amplification ratio (18) does not represent mere 1D effects, because it is calculated on the base of a 2D calculation. In deep or steep-sided valleys, topographical and 2D basin effects affect the response of the site at the centre. Consequently, the 2DCA coefficient (19) does not sum up the entire physical phenomena induced by 2D configurations. The main advantage of the 5-factor product (9) is that each aspect of 2D site effects is separated from the other, which can provide some physical explanations. Significant over-estimations are stated, but the accuracy of the five coefficients could be improved by using appropriate optimisation techniques. In this study, offset, filling, depth, slope and shape effects are quantified through rough maximizations. Correlations based on a statistical study could bring interesting improvements.

CONCLUSION

Site effects have been studied with the aid of “HYBRID”, a hybrid numerical program combining finite elements in the near field and boundary elements in the far field. Integrals in the domain are optimised by time truncation.

In engineering problems, it is useful to be able to predict the amplification ratio without using the heavy numerical simulation. Two evaluation techniques have been developed. A product of horizontal surface displacement amplification in five factors describes qualitatively and quantitatively the contributions of different parameters controlling site effects (offset, filling, depth, slope, shape). A “2D Combined Amplification” coefficient (2DCA coefficient) is defined to simplify the breakdown technique. It gives better quantitative results, and risks of amplification under-estimations are weak. In a nutshell, this 2DCA coefficient gives a quick approximation of 2D effects thanks to very accessible data.

Statistical post-treatment of data can improve the accuracy of the calculation methods developed to evaluate the amplification of horizontal displacements in two-dimensional irregular configurations. Other terms could be included in the breakdown, such as an exciting frequency ratio controlling the resonance type of the valley, or mechanical coefficient related to the impedance contrast.

REFERENCES

Bard, P.-Y.: “Diffracted waves and displacement field over two-dimensional elevated topographies”, Geophys. J. R. Astr. Soc., 71: 731-760, 1982

Bard and Bouchon, “The two-dimensional resonance of sediment-filled valleys”, Bulletin of the seismological society of America, 75(2) : 519-540, 1985

Bielak; Xu; Ghattos: “Earthquake Ground Motion and Structural Response in Alluvial Valleys”, Journal of Geotechnical and Geoenvironmental Engineering, 1999

Boore, D.M.; Harmsen, S.; Harding, S.: “Wave scattering from a steep change in surface topography”, Bulletin of the seismological society of America, 71: 117–125, 1981

Castellani, A; Peano, A.; Sardella, L.: “On analytical and numerical techniques for seismic analysis of topographic irregularities”, Proc. European Conf. Earthquake. Eng, 7th, Athens, Greece, 2: 415–423, 1982

Faccioli; Vanini; Frassine: “Complex Site Effects in Earthquake Ground Motion, Including Topography”, *Twelfth European Conference on Earthquake Engineering*, paper reference : 844, 2002

Gatmiri B. and Dehghan K. "Applying a new fast numerical method to elasto-dynamic transient kernels in HYBRID wave propagation analysis", EURODYN 2005, C. Soize & G.I. Schuëller (eds), 6th Conference on Structural Dynamics-EURODYN, Paris, Millpress, Rotterdam, pp. 1879-1884, September 2005

Gatmiri B. and Kamalian M. "Two-Dimensional Transient Wave Propagation in Anelastic Saturated Porous Media by a Hybrid FE/BE Method" 5th European Conference of Numerical Methods in Geotechnical Engineering, Paris, pp. 947-956, 2002a

Gatmiri B. and Kamalian M. "On the fundamental solution of dynamic poroelastic boundary integral equations in the time domain" International Journal of Geomechanics, 2(4) pp. 381-398, 2002b

Gatmiri B. and Nguyen K.V. "Time 2D Fundamental solution for Saturated Porous Media with Incompressible Fluid", International Journal of Communications in Numerical Methods in Engineering, 21: 119-132, 2005

Kawase, H.: “Time-domain response of a semicircular canyon for incident SV, P and Rayleigh waves calculated by the discrete wavenumber boundary element method”, Bulletin of the seismological Society of America, 78: 1415-1437, 1988

Luco; Barros: “3D Response of a Layered Cylindrical Valley Embedded in a Layered Half-Space”, Earthquake Engineering and Structural Dynamics, 24: 109 – 125, 1995

Nechtschein, S.; Bard, P.-Y.; Gariel, J.-C.; Meneroud, J.-P.; Dervin, P.; Cushing, M.; Gaubert, B.; Vidal, S.; Duval, A.-M.: “A topographic effect study in the Nice region”, Proceedings of the fifth international conference on seismic zonation, Nice, France, 1995, 1067-1074, 1995

Nguyen K.V. "Etude des effets de site dûs aux conditions topographiques et géotechniques par une méthode hybride éléments finis / éléments frontières", PhD dissertation, Ecole Nationale des Ponts et Chaussées, 2005, (in French)

Nguyen K.V. and Gatmiri B. "Evaluation of seismic ground motion induced by topographic irregularities", accepted for publication in International Journal of Soil Dynamics and Earthquake Engineering

Ohtsuki; Karumi: “Effects of Topography and Subsurface Inhomogeneities on Seismic SV Waves”, Earthquake Engineering and Structural Dynamics, 11: 441 – 462, 1983

Reinoso; Wrobel; Power: “3D Scattering of Seismic Waves from Topographical Structures”, Soil Dynamics and Earthquake Engineering, 16: 41 – 61, 1997

Sanchez-Sesma, F.J.; Herrera, I.; Aviles, J.: “A boundary method for elastic wave diffraction: application to scattering waves by surface irregularities”, Bulletin of the seismological Society of America, 72: 473-490, 1982

Trifunac, M.D.; Hudson DE.: “Analysis of the Pacoima Dam accelerogram - San Fernando, California, earthquake of 1971”, Bulletin of the seismological Society of America, 61: 1393-1411, 1971

Wong, H.; Jennings, P.: “Effect of canyon topographies on strong ground motion”, Bulletin of the seismological Society of America, 65:1239–1257, 1975